CORTEX 126 (2020) 63–72

Available online at www.sciencedirect.com

ScienceDirect

Journal homepage: www.elsevier.com/locate/cortex

Research Report

A graph theory study of resting-state functional connectivity in children with Tourette syndrome

Thaïra J.C. Openneer [a,*], Jan-Bernard C. Marsman [b], Dennis van der Meer [c], Natalie J. Forde [a,d], Sophie E.A. Akkermans [d,e], Jilly Naaijen [d,e], Jan K. Buitelaar [d,e,f], Andrea Dietrich [a,1] and Pieter J. Hoekstra [a,1]

[a] University of Groningen, University Medical Center Groningen, Department of Child and Adolescent Psychiatry, Groningen, the Netherlands

[b] Neuroimaging Center, Department of Neuroscience, University of Groningen, University Medical Center Groningen, Groningen, the Netherlands

[c] K.G. Jebsen Centre for Psychosis Research/Norwegian Centre for Mental Disorder Research (NORMENT), Institute of Clinical Medicine, University of Oslo, Oslo, Norway

[d] Karakter Child and Adolescent Psychiatry University Centre, Nijmegen, the Netherlands

[e] Radboud University Medical Center, Donders Institute for Brain, Cognition and Behaviour, Department of Cognitive Neuroscience, Nijmegen, the Netherlands

[f] Radboud University, Donders Institute for Brain, Cognition and Behaviour, Centre for Cognitive Neuroimaging, Nijmegen, the Netherlands

ARTICLE INFO

Article history:
Received 29 August 2019
Reviewed 14 November 2019
Revised 12 January 2020
Accepted 15 January 2020
Action editor Brad Dickerson
Published online 28 January 2020

Keywords:
Graph theoretical analysis
Resting-state fMRI
Tourette syndrome
Local efficiency
Default mode network
Tic severity
Comorbid ADHD

ABSTRACT

Little is known about the brain's functional organization during resting-state in children with Tourette syndrome (TS). We aimed to investigate this with a specific focus on the role of comorbid attention-deficit/hyperactivity disorder (ADHD). We applied graph theoretical analysis to resting-state functional magnetic resonance imaging data of 109 8-to-12-year-old children with TS ($n = 46$), ADHD without tics ($n = 23$), and healthy controls ($n = 40$). First, we compared these three groups, and in a second comparison four groups, distinguishing TS with (TS + ADHD, $n = 19$) and without comorbid ADHD (TS−ADHD, $n = 27$). Weighted brain graphs were constructed for both comparisons to investigate global efficiency, local efficiency, and clustering coefficient per acquired network. Local efficiency and clustering coefficient were significantly lower in children with TS−ADHD in the default mode network compared with healthy controls, and in the frontoparietal network compared with ADHD; we also found associations with higher tic severity. Our study supports a different functional brain network organization in children with TS−ADHD, compared with healthy controls and children with ADHD.

* *Corresponding author*. Department of Child and Adolescent Psychiatry, University Medical Center Groningen, Hanzeplein 1, 9713 GZ, Groningen, the Netherlands.
E-mail address: t.openneer@accare.nl (T.J.C. Openneer).

[1] Dietrich and Hoekstra share last authorship.

https://doi.org/10.1016/j.cortex.2020.01.006

1. Introduction

Tourette syndrome (TS) is a childhood-onset disorder, characterized by the presence of multiple motor and at least one vocal tic that have persisted for more than one year (Diagnostic and Satistical Manual of Mental Disorders, 2013). In recent years, the notion that neurodevelopmental disorders are associated with abnormal functional connectivity in large-scale brain networks has gained widespread acceptance (Zhang & Raichle, 2010). Resting-state functional magnetic resonance imaging (fMRI) captures undirected brain activity unrelated to a particular task, which enables the investigation of the full organization of the brain (Van den Heuvel & Hulshoff-Pol, 2010), and has been one of the fastest growing fields in neuroimaging over the past decade, applied in a variety of psychiatric disorders (Oldehinkel, Francx, Beckmann, Buitelaar, & Mennes, 2013; Rosazza & Minati, 2011). In TS, existing functional resting-state studies so far found significantly altered connectivity in frontoparietal areas relative to healthy controls (Church et al., 2009; Fan et al., 2018); these areas are implicated in multitasking and are thought to have an inhibitory role during inappropriate responses (Dosenbach et al., 2007). Additionally, a recent resting-state study in adults with TS observed low functional connectivity specifically in the default mode network, implicated in task-independent introspection or 'mind wandering', compared to healthy controls (Fan et al., 2018). However, despite the increasing use of resting-state studies, the functional brain organization in children with TS remains largely unknown given the sparse number of studies to date.

Recently, graph theoretical analysis emerged as an increasingly popular method for analyzing resting-state fMRI data, as it provides a powerful mathematical framework for the characterization of connections of brain functional networks (Bullmore & Sporns, 2009; Power et al., 2011). Brain networks are thought to be organized according to small-world architecture, depending on the developmental stage (Fair et al., 2009). Overall, anatomically close brain regions (nodes) have more connections (edges) than distant nodes, thereby satisfying the competitive demands of brain networks in information processing (Bullmore & Sporns, 2009). Therefore, graph theoretical analysis might be an important tool to unravel the underlying neural mechanisms of TS by investigating possible deviances in the topological brain organization.

Only a few existing resting-state studies to date used graph theoretical analysis to investigate the topological brain organization in TS. Studies that used graph theoretical analysis showed alterations in different networks of the brain compared with healthy controls. For instance, recently, Wen et al. (2018) observed a disrupted functional network organization in children and adolescents with TS relative to healthy controls in the default-mode areas. Furthermore, Church et al. (2009) observed an abnormal pattern of functional connections in the frontoparietal network in children with TS relative to age-matched healthy controls, suggesting an immature functional brain organization. Relatedly, Worbe et al. (2012) found functional changes in cortico-basal ganglia networks in adult TS patients compared with healthy adults. Overall, there seems to be evidence for an atypical topological brain organization in TS, especially in the default mode network and frontoparietal network.

However, the few existing studies are hampered by methodological challenges, making it difficult to compare between studies, such as the use of small sample sizes and wide age ranges. As the topological organization of the brain is thought to be dependent on the developmental stage (Fair et al., 2009; Power et al., 2011), brain organization investigated in adults may not be representative for the TS patient in childhood. Perhaps even more important, studies so far did not take attention-deficit/hyperactivity disorder (ADHD) comorbidity into account. This is a particular concern, as comorbid ADHD, occurring in about 50% of individuals with TS (Hirschtritt et al., 2015), is thought to play a predominant role in TS with regard to the functional organization of the brain. Indeed, in resting-state studies, similar deviant connectivity patterns in TS were found, specifically in the default mode network and frontoparietal network, in children with ADHD (without tics) in comparison with healthy controls (Castellanos et al., 2008; Marcos-Vidal et al., 2017; Tao et al., 2017). Currently, it remains unclear to what extent children with TS and ADHD show similar or dissimilar functional brain connectivity patterns as shown by the topological organization of the brain, and whether the frequently comorbid ADHD symptoms in TS might underlie possible functional connectivity abnormalities in TS versus controls or ADHD without tics.

In the present study, we therefore investigated the functional brain organization in 8-12-year-old children with TS with and without comorbid ADHD, ADHD without tics, and healthy controls. The age range of 8–12 years was chosen as tics are most prevalent at that age (Cohen, Leckman, & Bloch, 2013). We analyzed the data in two sets: first, we compared three groups of children: with TS irrespective of ADHD comorbidity, with ADHD without tics, and healthy controls; to allow for comparisons with the existing literature. Second, we compared four groups, distinguishing between TS with and without comorbid ADHD. We hypothesized that comorbid ADHD in TS would drive dissimilarities between TS and healthy controls, specifically, lower functional connectivity in the default mode network and frontoparietal network. Additionally, we investigated the graph measures in relation to tic and ADHD symptom severity. Due to the paucity of previous studies, we did not restrict our analyses to particular brain regions, but adopted a data-driven, whole-brain approach, using one of the largest sample sizes in a pediatric population to date.

2. Methods

We here report how we determined our sample size, all data exclusions, all inclusion/exclusion criteria, whether inclusion/exclusion criteria were established prior to data analysis, all manipulations, and all measures in the study. The conditions of our ethics approval do not permit public archiving of individual anonymized study data. Readers seeking access to the data should contact the Donders Institute for Brain,

Cognition and Behaviour, Radboud University Medical Center. Access will be granted to named individuals in accordance with ethical procedures governing the reuse of sensitive data. There are no further conditions.

2.1. Participants

A total of 128 children aged 8–12 years participated in this study, of whom 109 with usable functional resting-state data, including a group of children with TS ($n = 46$; $n = 19$ of whom had comorbid ADHD), with ADHD ($n = 23$), and healthy controls ($n = 40$). Nineteen children were excluded from the analyses due to excessive head motion ($n = 12$), low scan quality ($n = 6$), or an incidental finding ($n = 1$). There were no differences in group or symptom scores (tics or ADHD) between included and excluded children. The sample size was a priori determined. Affected children were recruited via child and adolescent psychiatry and neurology clinics and patient organizations throughout the Netherlands; healthy controls were recruited through local elementary schools. Inclusion criteria for the participants included Caucasian decent, as this study was part of a genetic cohort (see (Naaijen et al., 2016)), IQ > 70, no past or present head injuries, neurological disorders or major physical illness. Comorbid psychiatric conditions in TS and ADHD were allowed, except for obsessive-compulsive disorder (OCD) in the ADHD group, as this group was also part of a study on OCD (Naaijen et al., 2016). Healthy controls had to be free of any psychiatric disorder, as confirmed by the parent-administered Kiddie Schedule for Affective Disorders and Schizophrenia (K-SADS; https://www.pediatricbipolar.pitt.edu/resources/instruments (Kaufman et al., 1997)) based on DSM-IV-TR (Diagnostic and Satistical Manual of Mental Disorders, 2000) criteria administered to the parents, and by scores in the normal range on the Child Behavior Checklist and Teacher Report Form (CBCL and TRF; https://www.aseba.nl/home (Achenbach & Rescorla, 2001)). No part of the study procedures was pre-registered prior to the research being conducted. Children were asked to refrain from using stimulant medication 48 h prior to the testing day, which is an often-used wash-out period for stimulant drugs (Spencer et al., 2014), whereas other types of medication were allowed. Written informed consent was provided by the parents/guardians of the participant and by the child if 12 years of age; younger children provided oral assent. The study was approved by the regional ethics board (CMO Region Arnhem-Nijmegen).

2.2. Procedures and clinical measures

Diagnostic interviews, neuropsychological and fMRI assessments were carried out by trained investigators and took place during a single day. A chronic tic diagnosis according to DSM-IV-TR (Diagnostic and Satistical Manual of Mental Disorders, 2000) criteria was confirmed using the Yale Global Tic Severity Scale (YGTSS; https://www.kenniscentrum-kjp.nl/wp-content/uploads/2019/06/Vragenlijst-YGTSS-DCI.pdf (Leckman et al., 1989)), a semi-structured clinician-rated instrument that provides an inventory of the various past week motor and vocal tics (range 0–50). The clinical-rated Children's Yale-Brown Obsessive-Compulsive Scale (CY-BOCS; https://www.nji.nl/nl/Download-NJi/CY-BOCS-Vragenlijst-2009.pdf (Scahill et al., 1997)) was used to assess comorbid OCD. A clinical diagnosis of ADHD was confirmed by the K-SADS (Kaufman et al., 1997) based on DSM-IV-TR criteria. Moreover, all children with ADHD fell in the clinical range (all scores above the 97th percentile) as assessed by the TRF (Achenbach & Rescorla, 2001). Furthermore, the K-SADS was used to establish a diagnosis of oppositional defiant disorder (ODD) and conduct disorder (CD). To rate ADHD symptom count, the Conners' Parent Rating Scale – Revised Long version was used (CPRS-RL; https://mhs.com (Conners, Sitarenios, Parker, & Epstein, 1998)), capturing 18 DSM-IV-TR based ADHD symptoms (range 0–18).

2.3. MRI data acquisition

All children were scanned with a 3T Siemens Prisma scanner (Siemens, Erlangen, Germany) at the Donders Centre for Cognitive Neuroimaging in Nijmegen. The participants were allowed to practice in a dummy scanner. During scanning the lights were dimmed and a fixation cross was shown. Children were asked to lie still, not to fall asleep, and to keep their eyes open. Their heads were stabilized with cushions and tape to minimize movement during scanning. Tics were not monitored during the scanning. No more than one resting state run was acquired per person.

Anatomical images were acquired using a T1-weighted magnetization prepared rapid gradient echo (MPRAGE) sequence (TR = 2300 ms; TE = 2.98 ms; TI = 900 ms; Field of View = 256 mm; flip angle = 9°; slice thickness = 1.20 mm; in plane resolution 1.2 mm; T1 = 900 ms; acquisition time 5:30 min). The T2-weighted functional images during rest were acquired with a Multi-Echo Planar imaging sequence (TR = 2300 ms; TE1 = 12 ms; TE2 = 28.41 ms, TE3 = 44.82 ms; flip angle = 80°; matrix size 64 × 64; Field of view = 240 mm; 33 axial slices; descending slice acquisition; slice thickness = 3.8 mm with 10% gap, 215 volumes; in-plane resolution = 3.8 mm; bandwidth = 2442 Hz/pixel; iPAT factor 2; acquisition time 8:24 min).

2.4. Preprocessing of functional MRI images

First, functional images were converted to three Nifti filesets (one per TE) using dcm2nii (https://www.nitrc.org/projects/dcm2nii/; version 2may2016 (Rorden, Karnath, & Bonilha, 2007)). Subsequently, we applied multi-echo independent component analysis (ME-ICA, https://github.com/ME-ICA/me-ica; meica.py script version 2.5 (Kundu et al., 2013)) as a first step in denoising the BOLD signal without normalization options. This promising method has been demonstrated to remove complex non-BOLD artifacts, such as motion, by using TE dependence as a measure of BOLD signal (Kundu et al., 2013; Power et al., 2018), and allow a better separation of signal and noise in the time series (Power et al., 2018; Satterthwaite et al., 2019). The images were spatially realigned to correct and investigate residual head motion following ME-ICA, and subsequently co-registered to the anatomical T1 image of the subject. The images were normalized using DARTEL in SPM12 (Wellcome Department of Imaging Neuroscience, London, UK). DARTEL allows

groupwise normalization by iteratively defining an average template, based on all children in the three groups (3 × 3 × 3 mm isotropic voxels). This template is registered to MNI space, allowing the transformations to be combined so that all the individual spatially normalized scans can also be brought into MNI space. To remove sources of spurious variance, we applied regression of nuisance variables per gray-matter voxel, incorporating six rigid body head motion parameters, the global signal, white-matter (WM) signal, and cerebrospinal fluid (CSF) signal. To obtain the WM and CSF signals, we performed segmentation to create masks and extracted the first eigenvariate from the time-series of the included voxels. Thereafter, a bandpass filter was applied using a butterworth 9th order filter between .008 and .08 Hz. Smoothing was applied using a 4 mm full-width-at-half-maximum Gaussian kernel. Furthermore, we checked if volume censoring (scrubbing) was necessary as previously described in Power et al. (2012, 2018) to further minimize motion-related effects. Frame-by-frame head displacement (FD) was calculated from realignment estimates, and frame-by-frame signal change was calculated from the functional connectivity image generated after functional connectivity preprocessing. FD is calculated as the root of the sum of the squared derivatives of the movement parameters per volume, while DVARS is calculated as the root mean square of the derivatives of the time series across voxels included in the whole-brain mask per volume (Power et al., 2012). No volumes exceeded FD > .2 mm and/or DVARS >.5% (Power et al., 2012, 2018), thus no additional steps were necessary. Finally, we performed global signal regression, as this has shown to be an important denoising step for mitigating motion artifact (Power et al., 2018; Satterthwaite et al., 2019).

2.5. Group comparisons and network construction

We performed two sets of analyses. In the first set of our analyses, we compared children with TS ($n = 46$; irrespective of ADHD comorbidity), ADHD ($n = 23$), and healthy controls ($n = 40$). In the second set, we compared four groups (TS−ADHD $n = 27$, TS + ADHD $n = 19$, ADHD $n = 23$, healthy controls $n = 40$). The following steps were performed for each set.

In order to perform network statistics, brain parcellations were applied based on Power et al. (2011) yielding 264 regions of interest (ROIs) with 5 mm radius. To construct a connectivity matrix per subject, the regional mean time series for each of the 264 ROIs were extracted and Pearson correlations were calculated between all pairs. Correlations were set to zero if the distance between the centers of two ROIs was less than 20 mm (Geerligs, Renken, Saliasi, Maurits, & Lorist, 2015; Power et al., 2011; Servaas et al., 2015).

To enhance the contrast between strong and weak connectivity values, an optimal threshold was calculated using the method as described in Geerligs et al. (2015). First, correlation matrices were binarized using a range of proportional threshold values (retaining strongest .1% to the strongest 3% of connections, with an increment of .01%). Second, these matrices were averaged across subjects per threshold and the entropy was calculated for each of them to indicate for which threshold the edges showed the largest stability information-wise (lowest entropy). These results were compared to the results obtained via randomized matrices (for details, see (Geerligs et al., 2015)). The optimal threshold is the threshold where the original matrix shows the largest stability across subjects (lowest entropy) and where the difference in entropy is the largest between the original matrix and the average of the randomized matrices.

The optimal threshold for both analyses in our study was .0132. To achieve the optimal modular structure using the threshold of .0132, we first partitioned the nodes into networks, using the algorithm of Blondel, Guillaume, Lambiotte, & Lefebvre (2008), wherein nodes are divided in groups with a maximum number of within-group edges and a minimum number of between-group edges. This calculation was repeated 1000 times to increase the chance of escaping local maxima. Second, we applied the modularity fine-tuning algorithm of Sun, Danila, Josić, & Bassler (2009), wherein nodes are randomly assigned to other modules until modularity no further improves.

2.6. Graph metrics

Graph metrics (i.e., global efficiency, local efficiency and clustering coefficient) were calculated on weighted graphs for each network individually per group using the selected threshold, by using functions from the Brain Connectivity Toolbox (www.brain-connectivity-toolbox.net(Rubinov & Sporns, 2010)). We specifically chose for measures that are frequently used, to allow for comparisons with the literature.

2.6.1. Global efficiency

The global efficiency is the average inverse shortest path length (Latora & Marchiori, 2001). A short path length indicates that, on average, each node can reach other nodes with a path composed of only a few edges (Rubinov & Sporns, 2010). Thus, the global efficiency is one of the most elementary indicators of integration (i.e., the degree to which the network can share information between distributed regions).

2.6.2. Local efficiency

Local efficiency was measured as the average inverse shortest path length between a node and its direct neighbors (Rubinov & Sporns, 2010), which indicates the average efficiency of information transfer within neighborhoods.

2.6.3. Clustering coefficient

The clustering coefficient represents the fraction of triangles around a node and is equivalent to the fraction of the node's neighbors that are neighbors of each other (Rubinov & Sporns, 2010), thus indicating how close its neighbors tend to cluster together (Watts & Strogatz, 1998). Accordingly, the average clustering coefficient is considered as a direct measure of its segregation (i.e., the degree to which the network is organized into local specialized regions (Bullmore & Sporns, 2009)).

The measures chosen are indicative of how well children can process information within networks, i.e., how efficient they are in transferring information to neighboring regions (local efficiency) and remote regions (global efficiency), and how well they can process specialized information within densely interconnected groups of nodes (clustering

Table 1 – Group characteristics.

	HC($n = 40$)	TS($n = 46$)	TS−ADHD($n = 27$)	TS + ADHD($n = 19$)	ADHD($n = 23$)	Test Statistic	p-value	Direction
Male sex, n (%)	30 (75)	40 (87)	25 (92.6)	15 (78.9)	16 (69.6)	$\chi^2 = 3.51^a$	$p < .01$	TS > ADHD
						$\chi^2 = 3.52^a$	$p < .01$	TS-ADHD > ADHD
IQ (range)	106.3 ± 12.3 (80.6–129.1)	104.8 ± 12.0 (80.6–127.7)	105.9 ± 12.4 (80.6–127.7)	103.4 ± 11.6 (84.8–123.6)	102.8 ± 12.8 (70.9–123.6)			
Age, Years	10.9 ± 1.0	10.7 ± 1.3	10.7 ± 1.3	10.7 ± 1.4	11.0 ± 1.3			
Tic severity	–	22.5 ± 8.5	21.1 ± 7.5	24.5 ± 9.5	–			
ADHD symptom count	.6 ± 1.3	6.9 ± 4.6	4.7 ± 3.8	10.0 ± 3.8	9.4 ± 4.2	$F = 54.84^b$	$p < .01$	TS > HC TS-ADHD > HC TS + ADHD > HC ADHD > HC TS + ADHD > TS-ADHD ADHD > TS-ADHD
Comorbid diagnoses								
OCD, n	0	10	6	4	0			
ODD/CD, n	0	2	1	1	2			
Medication	0	6	3	3	3			

Values presented as n, percent or mean ± standard deviation. HC, healthy controls; TS, Tourette syndrome; ADHD, attention-deficit/hyperactivity disorder; TS-ADHD, TS without comorbid ADHD; TS + ADHD, TS with comorbid ADHD; OCD, obsessive-compulsive disorder; ODD/CD, oppositional defiant disorder/conduct disorder. Tic severity assessed by the Yale Global Tic Severity Scale (Leckman et al., 1989) (range 0–50); ADHD symptom count assessed by the Conners' Parent Rating Scale – Revised Long (Conners et al., 1998) (range 1–18). Medication denotes the number of children who were using medication during the testing day. Between-group differences were tested by a [a]Pearson's chi-squared test for males, and [b]an analysis of variance for ADHD symptom count; Non-significant results are not shown.

coefficient). By selecting these graph measures, we may unravel to what extent the information processing of children with TS and ADHD within networks are similar, and whether the frequently comorbid ADHD symptoms in TS might underlie possible atypical information processing in TS versus controls or ADHD without tics.

2.7. *Statistical analysis*

Differences in group characteristics were tested by an analysis of variance (ANOVA) for IQ, tic severity and ADHD symptom count, the non-parametric Mann–Whitney U test for age, and a Pearson's chi-square ($\chi 2$) test for sex, using SPSS version 23 (SPSS Inc., USA). An ANOVA was also used to test between-group differences in residual head motion after ME-ICA.

We investigated differences between groups in graph metrics (i.e., global efficiency, local efficiency and clustering coefficient) per network, using SPM12, implemented in Matlab 8.6.0. (The Mathworks Inc., Natick, MA). We applied non-parametric permutation testing, as we did not meet the assumptions for an ANOVA, where each measure was compared against a null distribution based on randomly permuted samples (1000 permutations). We chose these two separate sets of comparisons over a 2 × 2 factorial design as we argued that ADHD in the context of TS might differ from ADHD as such. We used a p-value of .025 on either direction to indicate significance.

In addition, linear regression analyses were performed in SPSS version 23 (SPSS Inc., USA), to investigate the relationship between graph measures and tic severity (using the total score of the YGTSS (Leckman et al., 1989)) in the TS sample ($n = 46$), and ADHD symptom count (using the CPRS-RL (Conners et al., 1998)) across the whole sample ($n = 109$), with age, sex and IQ included as covariates. No part of the study analyses was pre-registered prior to the research being conducted.

2.8. *Sensitivity analyses*

Furthermore, to remove potential influence of medication and gender, the analyses were subsequently re-done without the participants who used stimulant and non-stimulant medication during the test day, and without females. Additionally, we performed linear regression analyses between graph measures and ADHD severity in the TS and ADHD group only (excluding healthy controls).

3. Results

3.1. *Demographics*

See Table 1 for group characteristics. The TS group consisted of significantly more boys compared with the ADHD group. This was particularly true for TS–ADHD compared with ADHD. ADHD symptom count was lowest in healthy controls compared to the diagnostic groups, lower in TS–ADHD compared to TS + ADHD and ADHD, and not significantly different between the TS + ADHD and ADHD groups.

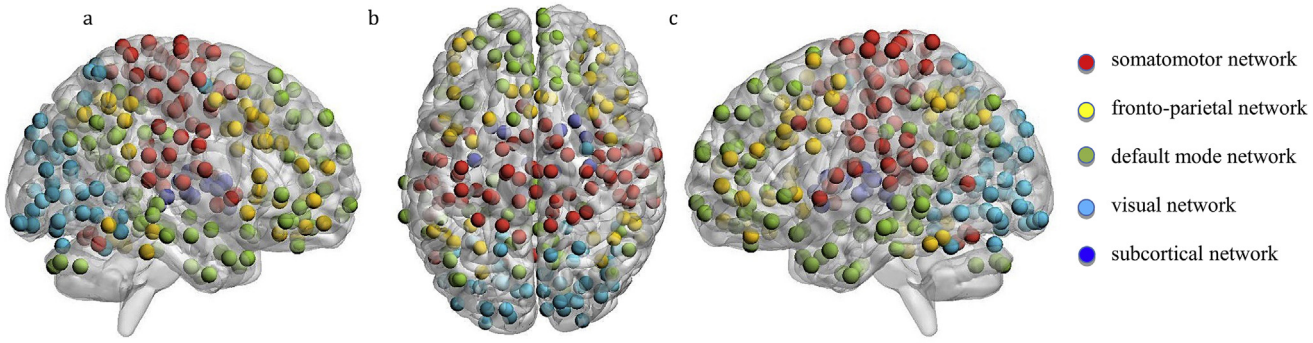

Fig. 1 – Module decomposition. Color indicate the different modules partitioned from the full sample of participants ($n = 109$). The nodes below to: somatomotor network (red; 69 nodes),fronto-parietal network (yellow; 49 nodes), default mode network (green; 87 nodes), visual network (light blue; 46 nodes), and subcortical network (dark blue; 13 nodes). Nodes are pasted overlaid on an inflated surface of the human brain using BrainNet viewer (Xia et al., 2013). Different views are shown: a.left side, b.top side, c.right side.

About 30% of the children with TS–ADHD, 50% of the children with TS + ADHD, and 70% of the children in the ADHD group without tics used medication in general (Supplement 1), that is stimulant and/or non-stimulant medication. Three children with ADHD did not comply with refraining from using stimulant medication 48 h prior to the testing day, while six children used non-stimulant medication during the testing day (antipsychotics: $n = 3$ children with TS–ADHD, $n = 2$ with TS + ADHD; clonidine: $n = 1$ child with TS + ADHD).

3.2. *Brain decomposition*

Five distinct modules emerged, as shown in Fig. 1: the somatomotor network, frontoparietal network, default mode network, visual network and subcortical network.

3.3. *Graph metrics*

The results for the graph metrics (i.e., global efficiency, local efficiency and clustering coefficient) are shown in Fig. 2 and Supplements 2 and 3. Lower local efficiency and clustering coefficient values were found in the default mode network for TS, specifically for TS–ADHD compared to healthy controls. Of note, the values for local efficiency and clustering coefficient in TS + ADHD were in a similar range of those with TS–ADHD and ADHD, and not of healthy controls.

Additionally, in our three-group comparison, comparing TS, ADHD, and healthy controls, we observed a significant difference between TS and ADHD in the frontoparietal network. Our four-group comparison revealed that specifically TS–ADHD showed significantly lower local efficiency

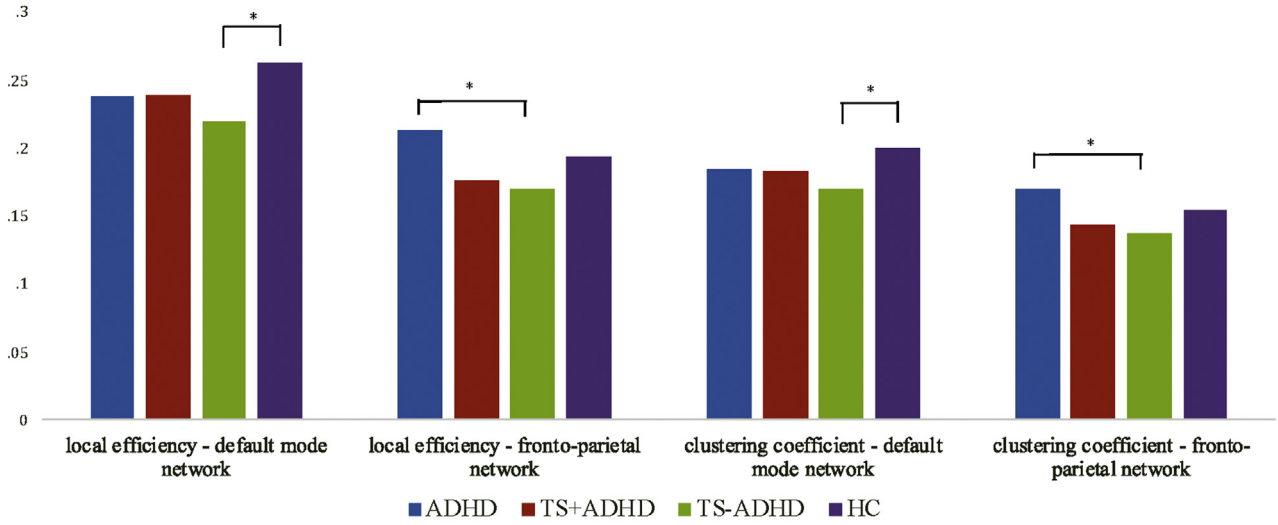

Fig. 2 – Result of local efficiency and clustering coefficients in the default mode network and fronto-parietal network between HC, TS-ADHD, TS+ADHD and ADHD. HC, healthy controls; TS, Tourette syndrome; ADHD, attention-deficit/hyperactivity disorder; TS-ADHD, TS without comorbid ADHD; TS + ADHD, TS with comorbid ADHD; a non-parametric permutation (1000 permutation) was used, therefore standard deviations are not applicable. *$p < .025$, see for additional network results of global efficiency, local efficiency and clustering coefficients Supplement 2.

Table 2 – Results of graph metrics in association with tic severity in the TS sample ($n = 46$) and ADHD symptoms in the total study sample ($n = 109$).

	Tic severity		ADHD severity	
	B ± SE	β	B ± SE	β
Global efficiency				
Somatomotor network	401.88 ± 391.16	.10	−74.00 ± 161.54	−.04
Fronto-parietal network	47.42 ± 377.42	.01	−58.15 ± 154.41	−.04
Default mode network	−132.43 ± 206.62	−.06	−185.29 ± 80.85	−.21
Visual network	157.90 ± 441.74	.03	−65.89 ± 180.93	−.03
Subcortical network	527.94 ± 1191.55	.04	−89.83 ± 489.01	−.02
Local efficiency				
Somatomotor network	−13.08 ± 15.22	−.08	3.79 ± 6.26	.06
Fronto-parietal network	−50.46* ± 18.50	−.25	7.81 ± 8.05	.09
Default mode network	−45.14* ± 23.73	−.19	5.74 ± 10.03	.06
Visual network	6.71 ± 13.14	.05	.54 ± 5.39	.01
Subcortical network	−3.84 ± 9.48	−.04	−.75 ± 3.89	−.02
Clustering coefficient				
Somatomotor network	−18.76 ± 19.31	−.09	4.28 ± 7.96	.05
Fronto-parietal network	−59.89* ± 24.38	−.22	11.95 ± 10.44	.11
Default mode network	−56.57* ± 31.48	−.17	9.63 ± 13.23	.07
Visual network	7.05 ± 16.53	.04	−1.16 ± 6.78	−.02
Subcortical network	−3.48 ± 10.57	−.03	−1.64 ± 4.33	−.04

B, unstandardized beta; SE, standard error for the unstandardized beta; β, standardized beta; TS, Tourette syndrome; ADHD, attention-deficit/hyperactivity disorder; tic severity assessed by the Yale Global Tic Severity Scale (Leckman et al., 1989) (range 0–50); ADHD symptom count assessed by the Conners' Parent Rating Scale – Revised Long (Conners et al., 1998) (range 1–18). Linear regression analyses were used, with age, sex IQ as covariates; *$p < .05$.

and lower clustering coefficient compared to ADHD. We observed no differences in global efficiency in our three-groups or four-groups analyses. Furthermore, we found no significant group differences in the somatomotor network, visual network or subcortical network in both sets of analyses. Finally, there were no differences in residual head motion between groups ($F[4,105] = 1.09$, $p = .82$).

3.4. *Dimensional analyses*

We observed a negative association between tic severity and local efficiency and clustering coefficient in the default mode network, and in the frontoparietal network (See Table 2 for results). No associations were observed between ADHD symptom count and network measures.

3.5. *Sensitivity analyses*

The results remained similar after excluding all females and medication-users during the testing-day from the analyses (Supplements 4 and 5). However, after removing healthy controls from the dimensional analyses, thus only using the TS and ADHD group, we observed a negative relation between global efficiency in the default mode network and ADHD severity, and a positive relation between local efficiency and clustering coefficient in the default mode network, and ADHD severity (Supplement 6).

4. Discussion

This study is among the first to investigate the functional brain organization using graph theoretical analysis in children with TS compared with healthy controls and ADHD, and to investigate the role of comorbid ADHD in TS. Overall, we observed a disrupted topological brain organization in TS, specifically decreased short-range connectivity in children with TS–ADHD in the default mode network compared with healthy controls, and in the frontoparietal network compared with children with ADHD; and in relation to higher tic severity.

We found support for low short-range network connectivity (lower local efficiency and clustering coefficient) in the default mode network in our TS group compared to healthy controls, specifically in TS–ADHD, and not TS + ADHD as we initially expected. Lower local efficiency is predominantly related to less efficient short-range connections between neighboring regions (Bullmore & Sporns, 2009), while lower clustering coefficient implies that the neighboring regions are less likely to be connected to each other, thereby indicating that they are less synchronized, more segregated, and more independent of each other, resulting in less efficient information transference (Rubinov & Sporns, 2010). The observed lower local efficiency and clustering coefficient in the default mode network of children with TS in our study are comparable with previously reported results of low resting-state connectivity of the default mode network in children and adults with TS (Cui et al., 2014; Wen et al., 2018), which may contribute to impaired task-independent introspection (mind wandering), such as thinking about the past (less efficient episodic memory), and impaired thinking about the future (e.g., planning (Buckner, Andrews-Hanna, & Schacter, 2008)). In contrast to Wen et al. (2018) we did not observe lower global efficiency (i.e., information transfer between remote regions) of default mode areas in children with TS. As the developmental stage of children influences the strength of

connections within the brain (Church et al., 2009; Fair et al., 2009), perhaps the broader age range of 3-16 years old children as used in Wen et al. (2018) as opposed to our restricted age range (8-12 years old children) may explain the discordant results. Interestingly, although not significantly different, the local efficiency and clustering coefficient of the default mode network in TS + ADHD appeared more similar to TS−ADHD than to healthy controls. Therefore, also given the association between higher tic severity and decreased local efficiency, our study supports that low local functional connectivity in the default mode network represents a TS-related deficit.

The frontoparietal network in our TS−ADHD group indicated also lower local efficiency and clustering coefficient compared to ADHD. Deviances of short-range connections in this network have been identified before by Church et al. (2009), indicating an immaturity ('a developmental delay') of the connections within the frontoparietal network of children and adolescents with TS (irrespective of comorbid ADHD) during resting-state, compared to their age-matched healthy peers. Healthy developing children are thought to have strongly correlated short-range functional connections (i.e., connections between regions close in space), that tend to decrease in strength over age, while long-range functional connections (i.e. connections between regions more distant in space) will increase in strength over age (Church et al., 2009; Fair et al., 2009). Connections showing a delay in development may therefore (temporarily) remain either too strong or too weak (Bos et al., 2017). The observed lower integration between short-range connections (i.e., low local efficiency) within both the default mode network and the frontoparietal network in TS in our study may therefore be indicative of an overall (immature) suboptimal neural functioning (Marcos-Vidal et al., 2017). While it should be noted that we did not find differences in the frontoparietal network compared with healthy controls, associations between higher tic severity and decreased local efficiency in both aforementioned networks may support our assumptions of maturational delay and an atypical functional brain network organization in TS. However, more research is warranted to corroborate these conclusions, and to elucidate relations with tic severity.

As mentioned, we observed higher local efficiency and clustering coefficient in the frontoparietal network in children with ADHD versus TS. Higher short-range connectivity in regions of the frontoparietal network in children with ADHD has been observed before compared to healthy controls (Bos et al., 2017; Marcos-Vidal et al., 2017), yet, other studies have observed lower short-range connectivity in the frontoparietal network (Lin, Tseng, Lai, Matsuo, & Gau, 2015; Tao et al., 2017). Regarding the default mode network, no differences between ADHD and the other groups were found in our study, despite previous findings (Castellanos et al., 2008; Marcos-Vidal et al., 2017; Tao et al., 2017). Discordant findings between studies may be explained by differences in age ranges and symptom severities, as our study included children with a restricted age range (between 8-12-year-old) with a relatively low ADHD symptom count (on average 9 out of 18 symptoms), suggesting a less severe ADHD group. Indeed, after removing healthy controls from our dimensional analyses, we observed associations in the default mode network between lower global efficiency values and higher ADHD severity, and between higher local efficiency and clustering coefficient in relation to higher ADHD severity, in line with previous observations (Lin et al., 2014; Wang et al., 2009). Overall, brain networks are thought to evolve to maximize the cost efficiency of parallel information processing (i.e., high efficiency of parallel information transfer at low costs (Sporns, Chialvo, Kaiser, & Hilgetag, 2004)). Therefore, ADHD symptoms (i.e., hyperactivity, inattention) may place aberrant demands on networks (e.g., frontoparietal and default mode network) to work as efficiently as possible, possibly resulting in a disorder-related shift of the network topology (Wang et al., 2009). Similarly, for TS, given the association between higher tic severity and lower short-range network connectivity, perhaps an altered network organization of both aforementioned networks is necessary to maximize the cost efficiency in the presence of (severe) tics. Evidently, the network architecture, specifically that of the frontoparietal network, seems to be disorder dependent, as shown in higher short-range connectivity values for ADHD and lower values for TS. Interestingly, however, given that the local efficiency and clustering values of the frontoparietal network for TS + ADHD were more similar to TS−ADHD than to those of ADHD, perhaps the presence of tics may be of more influence on the architecture of this specific network than the presence of ADHD symptoms, despite a similar ADHD symptom count in TS + ADHD and ADHD without tics. Nevertheless, future research is warranted to confirm these findings.

Strengths of this study were a sizeable sample of 8-12-year-old children with TS (with and without comorbid ADHD), ADHD without tics, and healthy controls. As we examined clinical groups where movement is often problematic, we specifically chose multi-echo independent component analysis, as it can robustly detect motion and other non-BOLD related signals, and implemented global signal regression (Kundu et al., 2013; Power et al., 2018). Limitations of this study included, first, the high percentage of males in the TS group compared with ADHD and the control group, and second, the use of stimulant and non-stimulant medication during the assessment day of a few participants. However, the results did not change after removing females or medication-users from the analyses. Third, as studies in tic suppression in adults with TS observed changes in control regions (Bohlhalter et al., 2006; Peterson et al., 1998), the possibility that some children may have suppressed their tics, might have influenced our results. Relatedly, while subtle tics may not necessarily cause motion artifacts, they may be associated with brain activation. Future research may benefit from careful monitoring of tics in the scanner. Fourth, other comorbid disorders apart from ADHD may have influenced our results. Unfortunately, the sample size did not allow for making corrections of these confounding factors. However, TS rarely presents by itself, and our sample composition reflects the complexities encountered in clinical practice (i.e., male predominance, use of medication, presence of comorbidities, suppression of tics).

In conclusion, we observed a different functional brain network organization in TS, specifically in TS−ADHD, compared to healthy controls and ADHD, and in relation to higher tic severity. This supports an overall suboptimal immature topological brain organization inherently related to

TS. Our study underlines the importance of future studies on resting-state connectivity in TS, preferably using larger samples and exploring the influence of comorbidities in TS, and furthermore to investigate the potential influence of tic severity on brain alterations in TS.

Declaration of Competing Interest

Jan K. Buitelaar has been in the past 3 years a consultant to/member of advisory board of/and/or speaker for Janssen Cilag BV, Eli Lilly, Shire, Medice, Lundbeck, Roche, and Servier. He is not an employee nor a stock shareholder of any of these companies. He has no other financial or material support, including expert testimony, patents or royalties. The other authors have no conflict of interest to report.

CRediT authorship contribution statement

Thaïra J.C. Openneer: Conceptualization, Methodology, Formal analysis, Writing - original draft. **Jan-Bernard C. Marsman:** Methodology, Software. **Dennis van der Meer:** Writing - review & editing. **Natalie J. Forde:** Investigation, Writing - review & editing. **Sophie E.A. Akkermans:** Investigation, Writing - review & editing. **Jilly Naaijen:** Investigation, Writing - review & editing. **Jan K. Buitelaar:** Conceptualization, Writing - review & editing. **Andrea Dietrich:** Conceptualization, Investigation, Methodology, Writing - review & editing, Supervision. **Pieter J. Hoekstra:** Conceptualization, Methodology, Writing - review & editing, Supervision.

Acknowledgments

This work was supported by the European Community's Sevent Framework Programme FP7/2007–2013 [grant number 278948] (TACTICS); and FP7-PEOPLE-2012-ITN [grant number 316978] (TS-EUROTRAIN). This manuscript reflects only the authors' view and the European Union is not liable for any use that may be made of the information contained herein.

Supplementary data

Supplementary data to this article can be found online at https://doi.org/10.1016/j.cortex.2020.01.006.

REFERENCES

Achenbach, T. M., & Rescorla, L. A. (2001). *Manual for the ASEBA school-age forms & profiles*. Burlington, VT: University of Vermont, Research Center for Children, Youth, & Families.

American Psychiatric Association. (2000). *Diagnostic and satistical manual of mental disorders* (4th ed.). TR Washington, DC: American Psychiatric Press.

American Psychiatric Association. (2013). *Diagnostic and satistical manual of mental disorders* (5th ed.). Washington, DC: American Psychiatric Press.

Blondel, V. D., Guillaume, J. L., Lambiotte, R., & Lefebvre, E. (2008). Fast unfolding of communities in large networks. *Journal of Statistical Mechanics, 10*, P100008.

Bohlhalter, S., Goldfine, A., Matteson, S., Garraux, G., Hanakawa, T., Kansaku, K., et al. (2006). Neural correlates of tic generation in tourette syndrome: An event- related functional MRI study. *Brain, 129*, 2029–2037.

Bos, D. J., Oranje, B., Achterberg, M., Vlaskamp, C., Ambrosino, S., De Reus, M. A., et al. (2017). Structural and functional connectivity in children and adolescents with and without attention deficit/hyperactivity disorder. *Journal of Child Psychology and Psychiatry, 58*, 810–818. https://doi.org/10.1111/jcpp.12712.

Buckner, R. L., Andrews-Hanna, J. R., & Schacter, D. L. (2008). The brain's default network: Anatomy, function, and relevance to disease. *Annals of the New York Academy of Sciences, 1124*, 1–38. https://doi.org/10.1196/annals.1440.011.

Bullmore, E., & Sporns, O. (2009). Complex brain networks: Graph theoretical analysis of structural and functional systems. *Nature Reviews. Neuroscience, 10*, 186–198. https://doi.org/10.1038/nrn2575.

Castellanos, F. X., Margulies, D. S., Kelly, C., Uddin, L. Q., Ghaffari, M., Kirsch, A., et al. (2008). Cingulate-precuneus interactions: A new locus of dysfunction in adult attention-deficit/hyperactivity disorder. *Biological Psychiatry, 63*, 332–337.

Church, J. A., Fair, D. A., Dosenbach, N. U. F., Cohen, A. L., Miezin, F. M., Petersen, S. E., et al. (2009). Control networks in paediatric Tourette syndrome show immature and anomalous patterns of functional connectivity. *Brain, 132*, 225–238. https://doi.org/10.1093/brain/awn223.

Cohen, S. C., Leckman, J. F., & Bloch, M. H. (2013). Clinical assessment of Tourette syndrome and tic disorders. *Neuroscience and Biobehavioral Reviews, 37*, 997–1007. https://doi.org/10.1016/j.neubiorev.2012.11.013.

Conners, C. K., Sitarenios, G., Parker, J. D. A., & Epstein, J. N. (1998). The revised connors' parent rating scale (CPRS-R): Factor structure, reliability, and criterion validity. *Journal of Abnormal Child Psychology, 26*, 257–268.

Cui, Y., Jin, Z., Chen, X., He, Y., Liang, X., & Zheng, Y. (2014). Abnormal baseline brain activity in drug-naïve patients with tourette syndrome: A resting-state fMRI study. *Frontiers in Human Neuroscience, 7*, 913. https://doi.org/10.3389/fnhum.2013.00913.

Dosenbach, N. U. F., Fair, D. A., Miezin, F. M., Cohen, A. L., Wenger, K. K., Dosenbach, R. A. T., et al. (2007). Distinct brain networks for adaptive and stable task control in humans. *Proceedings of the National Academy of Sciences of the United States of America, 104*, 11073–11078.

Fair, D. A., Cohen, A. L., Power, J. D., Dosenbach, N. U. F., Church, J. A., Miezin, F. M., et al. (2009). Functional brain networks develop from a "local to distributed" organization. *Plos Computational Biology, 5*, e1000381. https://doi.org/10.1371/journal.pcbi.1000381.

Fan, S., van den Heuvel, O. A., Cath, D. C., de Wit, S. J., Vriend, C., Veltman, D. J., et al. (2018). Altered functional connectivity in resting state networks in Tourette's disorder. *Frontiers in Human Neuroscience, 12*, 363. https://doi.org/10.3389/fnhum.2018.00363.

Geerligs, L., Renken, R. J., Saliasi, E., Maurits, N. M., & Lorist, M. M. (2015). A brain-wide study of age-related changes in functional connectivity. *Cerebral Cortex, 25*, 1987–1999. https://doi.org/10.1093/cercor/bhu012.

Hirschtritt, M. E., Lee, P. C., Pauls, D. L., Dion, Y., Grados, M. A., Illmann, C., et al. (2015). Lifetime prevalence, age of risk, and etiology of comorbid psychiatric disorders in Tourette syndrome. *JAMA Psychiatry, 72*(4), 325–333. https://doi.org/10.1001/jamapsychiatry.2014.2650.

Kaufman, J., Birmaher, B., Brent, D., Rao, U., Flynn, C., Moreci, P., et al. (1997). Schedule for affective disorders and Schizophrenia for school-age children-present and lifetime version (K-SADS-PL): Initial reliability and validity data. *Journal*

of the American Academy of Child and Adolescent Psychiatry, 36, 980–988.
Kundu, P., Brenowitz, N. D., Voon, V., Worbe, Y., Vértes, P. E., Inati, S. J., et al. (2013). Integrated strategy for improving functional connectivity mapping using multiecho fMRI. Proceedings of the National Academy of Sciences of the United States of America, 110, 16187–16192. https://doi.org/10.1073/pnas.1301725110.
Latora, V., & Marchiori, M. (2001). Efficient behavior of small-world networks. Physical Review Letters, 87, 198701.
Leckman, J. F., Riddle, M. A., Hardin, M. T., Ort, S. L., Swartz, K. L., Stevenson, J., et al. (1989). The Yale global tic severity scale: Initial testing of a clinician-rated scale of tic severity. Journal of the American Academy of Child and Adolescent Psychiatry, 28, 566–573.
Lin, P., Sun, J., Yu, G., Wu, Y., Yang, Y., Liang, M., et al. (2014). Global and local brain network reorganization in attention-deficit/hyperactivity disorder. Brain Imaging and Behavior, D8(4), 558–569.
Lin, H. Y., Tseng, W. Y., Lai, M. C., Matsuo, K., & Gau, S. S. (2015). Altered resting-state frontoparietal control network in children with attention-deficit/hyperactivity disorder. Journal of the International Neuropsychological Society, 21, 271–284. https://doi.org/10.1017/S135561771500020X.
Marcos-Vidal, L., Martinez-Garcia, M., Pretus, C., Garcia-Garcia, D., Martinez, K., Janssen, J., et al. (2017). Local functional connectivity suggests functional immaturity in children with attention-deficit/hyperactivity disorder. Human Brain Mapping, 39, 2442–2454. https://doi.org/10.1002/hbm.24013.
Naaijen, J., de Ruiter, S., Zwiers, M. P., Glennon, J. C., Durston, S., Lythgoe, D. J., et al. (2016). COMPULS: Design of a multicenter phenotypic, cognitive, genetic, and magnetic resonance imaging study in children with compulsive syndromes. BMC Psychiatry, 16, 361.
Naaijen, J., Forde, N. J., Lythgoe, D. J., Akkermans, S. E. A., Openneer, T. J. C., Dietrich, A., et al. (2016). Fronto-striatal glutamate in children with Tourette's disorder and attention-deficit/hyperactivity disorder. NeuroImage Clinics, 13, 16–23. https://doi.org/10.1016/j.nicl.2016.11.013.
Oldehinkel, M., Francx, W., Beckmann, C. F., Buitelaar, J. K., & Mennes, M. (2013). Resting state FMRI research in child psychiatric disorders. European Child & Adolescent Psychiatry, 22, 757–770. doi:0.1007/s00787-013-0480-0.
Peterson, B. S., Skudlarski, P., Anderson, A. W., Zhang, H., Gatenby, J. C., Lacadie, C. M., et al. (1998). A functional magnetic resonance imaging study of tic suppression in Tourette syndrome. Archives of General Psychiatry, 55, 326–333.
Power, J. D., Barnes, K. A., Snyder, A. Z., Schlaggar, B. L., & Petersen, S. E. (2012). Spurious but systematic correlations in functional connectivity MRI networks arise from subject motion. Neuroimage, 59, 2142–2154. https://doi.org/10.1016/j.neuroimage.2011.10.018.
Power, J. D., Cohen, A. L., Nelson, S. M., Wig, G. S., Barnes, K. A., Church, J. A., et al. (2011). Functional network organization of the human brain. Neuron, 72, 665–678. https://doi.org/10.1016/j.neuron.2011.09.006.
Power, J. D., Plitt, M., Gotts, S. J., Kundu, P., Voon, V., Bandettini, P. A., et al. (2018). Ridding fMRI data of motion-related influences: Removal of signals with distinct spatial and physical bases in multiecho data. Proceedings of the National Academy of Sciences of the United States of America, 115, E2105–E2114. https://doi.org/10.1073/pnas.1720985115.
Rorden, C., Karnath, H. O., & Bonilha, L. (2007). Improving lesion-symptom mapping. Journal of Cognitive Neuroscience, 19, 1081–1088.
Rosazza, C., & Minati, L. (2011). Resting-state brain networks: Literature review and clinical applications. Journal of the Neurological Sciences, 32, 773–785. https://doi.org/10.1007/s10072-011-0636-y.
Rubinov, M., & Sporns, O. (2010). Complex network measures of brain connectivity: Uses and interpretations. Neuroimage, 52, 1059–1069. https://doi.org/10.1016/j.neuroimage.2009.10.003.
Satterthwaite, T. D., Ciric, R., Roalf, D. R., Davatzikos, C., Bassett, D. S., & Wolf, D. H. (2019). Motion artifact in studies of functional connectivity: Characteristics and mitigation strategies. Human Brain Mapping, 40, 2033–2051. https://doi.org/10.1002/hbm.23665.
Scahill, L., Riddle, M. A., McSwiggin-Hardin, M., Ort, S. I., King, R. A., Goodman, W. K., et al. (1997). Children's Yale-Brown obsessive-compulsive scale: Reliability and validity. Journal of the American Academy of Child and Adolescent Psychiatry, 36, 844–852.
Servaas, M. N., Geerligs, L., Renken, R. J., Marsman, J. B., Ormel, J., Riese, H., et al. (2015). Connectomics and neuroticism: An altered functional network organization. Neuropsychopharmacology, 40, 296–304. https://doi.org/10.1038/npp.2014.169.
Spencer, T. J., Brown, A., Seidman, L. J., Valera, E. M., Makris, N., Lomedico, A., et al. (2014). Effect of psychostimulants on brain structure and function in ADHD: A qualitative literature review of MRI-based neuroimaging studies. Journal of Clinical Psychiatry, 74, 902–917. https://doi.org/10.4088/JCP.12r08287.
Sporns, O., Chialvo, D. R., Kaiser, M., & Hilgetag, C. C. (2004). Organization, development and function of complex brain networks. Trends in Cognitive Sciences, 8(9), 418–425.
Sun, Y., Danila, B., Josić, K., & Bassler, K. E. (2009). Improved community structure detection using a modified fine-tuning strategy. Europhysics Letters, 86, 28004.
Tao, J., Jiang, X., Wang, X., Liu, H., Qian, A., Yang, C., et al. (2017). Disrupted control-related functional brain networks in drug-naive children with attention-deficit/hyperactivity disorder. Frontiers in Psychiatry, 8, 246. https://doi.org/10.3389/fpsyt.2017.00246.
Van den Heuvel, M. P., & Hulshoff-Pol, H. E. (2010). Exploring the brain network: A review on resting-state fMRI functional connectivity. European Neuropsychopharmacology, 20, 519–534. https://doi.org/10.1016/j.euroneuro.2010.03.008.
Wang, L., Zhu, C., He, Y., Zang, Y., Cao, Q., Zhang, H., et al. (2009). Altered small-world brain functional networks in children with attention-deficit/hyperactivity disorder. Human Brain Mapping, 30, 638–649.
Watts, D. J., & Strogatz, S. H. (1998). Collective dynamics of 'small-world' networks. Letter Nature, 393, 440–442.
Wen, H., Liu, Y., Rekik, I., Wang, S., Chen, Z., Zhang, J., et al. (2018). Combining disrupted and discriminative topological properties of functional connectivity networks as neuroimaging biomarkers for accurate diagnosis of early Tourette syndrome children. Molecular Neurobiology, 55, 3251–3269. https://doi.org/10.1007/s12035-017-0519-1.
Worbe, Y., Malherbe, C., Hartmann, A., Pélégrini-Issac, M., Messé, A., Vidailhet, M., et al. (2012). Functional immaturity of cortico-basal ganglia networks in Gilles de la Tourette syndrome. Brain, 135, 1937–1946. https://doi.org/10.1093/brain/aws056.
Xia, M., Wang, J., & He, Y. (2013). BrainNet viewer: A network visualization tool for human brain connectomics. Plos One, 8, e68910. https://doi.org/10.1371/journal.pone.0068910.
Zhang, D., & Raichle, M. E. (2010). Disease and the brain's dark energy. Nature Reviews. Neurology, 6, 15–28. https://doi.org/10.1038/nrneurol.2009.198.